Conservative and Nonconservative Torques in Optical Binding

D. Haefner, S. Sukhov, and A. Dogariu

CREOL, The College of Optics and Photonics, University of Central Florida, Orlando, Florida 32816-2700, USA

(Received 17 July 2009; published 21 October 2009)

We show that in the canonical case of two lossless spheres that are electromagnetically coupled there is interplay between conservative and nonconservative forces, which is controlled by the polarization of the bounding field. We demonstrate that this phenomenon leads to new mechanisms to induce torques on spherically symmetric, optically isotropic, and lossless objects. The electromagnetic interaction can be exploited to apply orbital torque about the mutual center of mass of the bounded spheres as well as spin around the individual axes. When the incident field is linearly polarized, the torques are mostly conservative and affect only transient behaviors while for circularly polarized fields, the torques are entirely nonconservative, resulting in steady rotations. Means to control the magnitudes of orbital and spin torques are presented and applications to nanorotator machines are discussed.

DOI: 10.1103/PhysRevLett.103.173602 PACS numbers: 42.50.Wk, 42.25.Fx

The idea of a mechanical action of light has been pursued for hundreds of years. The ability to trap and maneuver small objects such as microparticles, polymer chains, cells, etc., is undoubtedly one of the most exciting uses of what is now commonly referred to as optical tweezers [1]. A host of applications are being pursued where optical forces are employed for manipulation, measurements, or for creating and controlling new states of matter. For instance, one important consequence of electromagnetic particle-particle interaction is the optical binding (OB) first noted by Burns *et al.* [2]. Two particles excited by a common field can form a bound ''optical dimer'' when they arrange themselves to a stable position where the radial forces acting on them are zero.

Since the first OB demonstration, a number of aspects have been studied including the excitation generated by counterpropagating beams [3], effects of the beams' structure [4], or the consequences of scattering [5]. In all situations, the resultant binding intrinsically depends on the potential energy landscape created by the conservative part of the electromagnetic forces.

A fundamental consequence of an applied force is the ability to induce torque with respect to some reference point. Torques can also be induced by optical fields. Several concepts for optical spin motors or ''nanorotators'' have been discussed based on optical traps created with circularly polarized light or vortex beams and relying on an object's asymmetry, absorption, or birefringence [6–8]. Another notable proposal uses the subtle interplay between conservative and nonconservative forces in an optical trap to create a ''nanofountain'' with a constant circulation of trapped particles [9].

In this Letter we introduce a new mechanism to generate optical torques. Electromagnetic fields can induce conservative forces resulting from field gradients as well as nonconservative forces appearing due to radiation pressure and gradients of phase. We show that in the case of OB particles, these forces determine conservative and nonconservative torques and, most importantly, the interplay between them is controlled by the polarization of the incident field.

Let us examine the system of two identical spherical particles illuminated by a plane wave propagating perpendicularly to the radius vector connecting the centers of the particles, as shown in Fig. 1. Forces are generated on the spheres due to the three-dimensional, polarized field established as a result of scattering [10]. Because of symmetry in the xy plane, the force acting on each particle can be decomposed into radial (binding) and tangential (rotational) components. There is also a scattering force along the incident wave wave vector $\mathbf{k}$, but its effect is identical for the two particles and does not hamper their transversal movement. This is the classical OB geometry [2,11,12].

In the simplest case of bound Rayleigh particles, the force acting on one scatterer can be estimated as

$$\langle F_u \rangle = \frac{1}{2}\,\mathrm{Re}\left(\alpha^* \mathbf{E}^* \frac{\partial \mathbf{E}}{\partial u}\right), \tag{1}$$

where α is the scatterer's polarizability, $\mathbf{E}$ is the electric field, $u = x, y, z$, and $*$ denotes complex conjugate. The

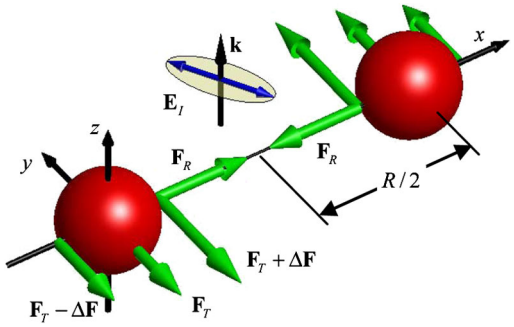

FIG. 1 (color online). Optical binding in elliptically polarized light. Apart from the binding force $\mathbf{F}_R$, interacting particles experience tangential forces $\mathbf{F}_T$. Note the existence of differential forces $\Delta\mathbf{F}$ leading to individual spinning in addition to common orbiting of particles around the system's center of mass.

field $\mathbf{E}$ is found by solving self-consistently the system of equations that takes into account the mutual interaction between the particles [11]

$$\begin{aligned}\mathbf{E}(\mathbf{r}_1) &= \mathbf{E}_I(\mathbf{r}_1) + \mathbf{G}\alpha\mathbf{E}(\mathbf{r}_2),\\ \mathbf{E}(\mathbf{r}_2) &= \mathbf{E}_I(\mathbf{r}_2) + \mathbf{G}\alpha\mathbf{E}(\mathbf{r}_1).\end{aligned} \tag{2}$$

In Eq. (2), $\mathbf{r}_1$ and $\mathbf{r}_2$ represent the dipole locations, $\mathbf{E}_I(\mathbf{r})$ is the incident field, and the tensor $\mathbf{G}(|\mathbf{r}_1 - \mathbf{r}_2|)$ is the interdipole propagator. The field derivative is then calculated to obtain the final expression for the force in Eq. (1).

A popular way for evaluating the derivative $\partial\mathbf{E}/\partial u$ is to differentiate the final solution of the system of Eqs. (2) [see Eq. (4) in Ref. [11]]. By doing so, however, the results contradict the calculation of time-averaged forces based on the well-established formalism of momentum flux tensor (Maxwell stress tensor) [14]. The correct way of evaluating the derivative $\partial\mathbf{E}/\partial u$ is to differentiate with respect to either $\mathbf{r}_1$ or $\mathbf{r}_2$ directly in Eq. (2). It is interesting to note that the way $\partial\mathbf{E}/\partial u$ is calculated has a minor effect for the radial, binding force; this is perhaps the reason this inconsistency has not been noticed before. When evaluating the tangential forces, however, there are situations where the way the calculation of field derivatives is conducted becomes important as it will be demonstrated here.

Using Eqs. (1) and (2) one can now evaluate the radial and tangential forces to be

$$\langle F_R\rangle = \frac{|\alpha|^2}{2}\left[\frac{|E_\parallel^I|^2}{|1-\eta\alpha|^2}\mathrm{Re}\left(\frac{\partial\eta}{\partial r}\right) + \frac{|E_\perp^I|^2}{|1-\mu\alpha|^2}\mathrm{Re}\left(\frac{\partial\mu}{\partial r}\right)\right], \tag{3a}$$

$$\langle F_T\rangle = |\alpha|^2\mathrm{Re}\left(\frac{\eta-\mu}{R}\right)\mathrm{Re}\left(\frac{E_\parallel^{I^*}E_\perp^I}{(1-\eta^*\alpha^*)(1-\mu\alpha)}\right), \tag{3b}$$

where $\eta = 2\exp(ikR)(-ikR+1)/R^3$ and $\mu = \exp(ikR)(k^2R^2 + ikR - 1)/R^3$ are eigenvalues of $\mathbf{G}$, $R = |\mathbf{r}_1 - \mathbf{r}_2|$, and k is the wave number. $E_\perp^I$, $E_\parallel^I$ are the components of incident field perpendicular and parallel to the separation vector. We can now proceed to examine the effect of the incident polarization.

Optical binding with linearly polarized light.—Because the depth of the potential wells in the stationary points depends on the incident polarization [12], the system of optically bound particles tends to orient itself such that it occupies the most energetically favorable position. When the interaction is weak ($\eta\alpha \ll 1$, $\mu\alpha \ll 1$), Eq. (3b) simplifies to $\langle F_T\rangle = |\alpha|^2|\mathbf{E}_I|^2\cos(2\theta)\mathrm{Re}[(\eta-\mu)/R]$, where θ is the angle between polarization and separation vectors. We note that the tangential force varies in space proportionally to $\cos(kR)$ or $\sin(kR)$ having the same periodicity as the radial (binding) force [Eq. (3a)]. The tangential force acting on a dipolelike particle is zero when the field polarization is along or orthogonal to the separation vector.

For systems of larger particles one has to go beyond the simple dipole approximation and use numerical procedures. The method of choice is the coupled dipole approximation (CDA). We use an extension of CDA that accounts for the interaction between particles without discretizing of space between them [15]. The calculations yield the local field distribution from which the forces acting on each individual dipoles are found using the procedure described in Ref. [16]. Subsequently, one may readily find the corresponding torques $\mathbf{\Gamma}_T = \sum_j \mathbf{R}_j^\perp \times \mathbf{F}_T(r_j) + \mathbf{p}_j^\perp \times \mathbf{E}_\perp(\mathbf{r}_j)$ by summing over all dipoles $\mathbf{p}_j$ in the system [17]. Here $\mathbf{R}_j$ represents the position of the dipole relative to the axis of rotation and the symbol $\perp$ denotes the components of vectors perpendicular to the chosen axis. In the case of OB spheres, one may identify torques resulting in two special rotational motions: (i) spheres orbiting together around their common center of mass and (ii) spheres spinning about their own axis.

Typical results of CDA calculations are illustrated in Fig. 2. As can be seen, there are no torques when the incident polarization is orthogonal or along the separation vector. However, torques arise at any other angle resulting in orbital and spin motions. Note that the torque does not reach its maximum at exactly $\theta = \pi/4$ as may have been expected. The reason is that the separation vector corresponding to a stable binding position is also a function of angle θ [12]. The unexpected appearance of spin torque is due to a gradient in the tangential force across the spheres as shown in Fig. 1. Because of this gradient the spin torque has an opposite sign compared to the orbital one. In fact, the mere existence of these spin torques is a significant result, demonstrating that OB interaction can lead to rotations of lossless dielectric objects.

The torques in Fig. 2 are mostly determined by gradient forces and, hence, determined by the conservative part of the total force. In any system with damping, the mechanical motion created by a conservative force will eventually cease, and the OB particles will align perpendicular to the direction of polarization. In the following we will reveal other situations where the nonconservative forces are the main cause for such torques.

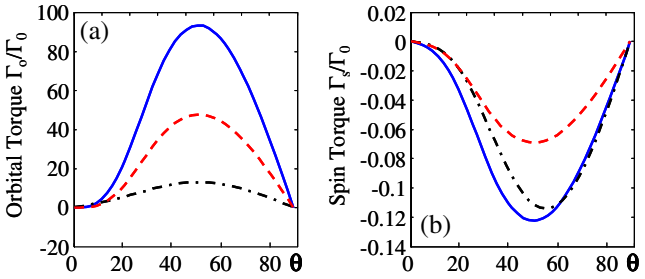

FIG. 2 (color online). Torques in an optically bound system of silica spheres of radius $a = 0.1\lambda_m$ solid lines, $a = 0.2\lambda_m$ dashed lines, $a = 0.4\lambda_m$ dot-dashed lines: (a) orbital torque about the system's center of mass and (b) spin torque of a sphere about its own axis. The spheres are in water and are excited with a field polarized linearly at an angle θ with respect to the optical binding vector ($\Gamma_0 = 10^4|\mathbf{E}_I|^2a^4/\lambda$).

Optical binding with circularly polarized light.— Recently, we demonstrated that scattering of circularly polarized light from a sphere generates a spiraling energy flow around it [18]. This effect arises from the conversion of spin angular momentum of incident light into orbital angular momentum of scattered light. One can envision that a test object placed in the vicinity of such a sphere will experience the radiation pressure from the curved power flow, causing the object to move along curled trajectory. In reality, the situation is complicated by the interaction between the two bodies as was discussed before. Moreover, together with radiation pressure, the field gradient force and the force due to gradient of phase may play a significant role. Thus, the real outcome can only be found by analyzing self-consistently the problem of electromagnetic interaction.

Starting from Eq. (3b) in the simple case of small nonabsorbing dielectric particles, the tangential force can be approximated to be [19]

$$\langle F_T \rangle = \pm |\alpha|^2 \mathrm{Re}(\alpha) |\mathbf{E}_I|^2 [6kR(3 - k^2R^2)\cos(2kR) - (9 - 15k^2R^2 + k^4R^4)\sin(2kR)]/4R^7. \quad (4)$$

The sign is determined by the polarization's handedness. It is worth noting that the force magnitude changes as a function of R with twice the frequency compared to the optical binding force evaluated from Eq. (3a). Furthermore, contrary to the case of linear excitation, the potential landscape is now circularly symmetric as shown in the inset of Fig. 3. This means that the tangential forces are completely nonconservative and create a steady-state orbital torque about the system's center of mass. Particles move along stationary orbits with radii determined by the condition $\langle F_R \rangle = 0$. In addition to this continuous rotation around the common axis, the particles will also exhibit a continuous rotation around their own axes due to the gradient of the nonconservative tangential force along the radial direction.

A typical summary plot of the orbital torque is shown in Fig. 3. Also shown are the analytical predictions of Eq. (4) for Rayleigh particles, which seem to make a good description up to a radius of about a tenth of the wavelength. As apparent in Fig. 3, an interesting effect occurs for larger spheres: the orbital rotation can change its sense depending on the particle size. This change in the direction of rotation, not present in the case of small particles, can happen even when moving between the different stationary orbits. Our calculations also indicate that for particles with $a \approx \lambda_m$, the radial and tangential forces have now similar periodicities as a function of R and, moreover, the zeros of radial force and the zeros of the tangential force occur approximately in the same place. Thus, a slight modification in the radial position of spheres can change the direction of rotation.

In addition to electromagnetic interaction, OB systems can also be subject to Brownian motion. Directional motion due to optical forces will be affected by the additional chaotic movement associated with some random force $\langle F_B^2 \rangle = 12\pi\eta a k_B T$ [20]. The torque resulting from the Brownian force provides a useful reference for the magnitude of orbital torques. In Fig. 3, one can clearly see that for $a \geq 0.3\lambda_m$ and an optical intensity of 50 mW/μm^2, the optically induced torques dominate.

Because of the complex interaction, the OB particles are also subject to spin torque with respect to the individual axes as shown in Fig. 4. As can be seen, for the chosen

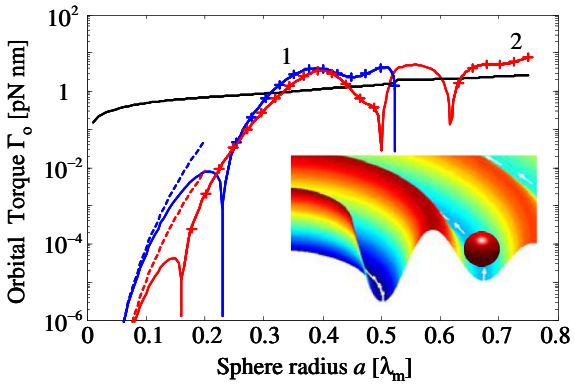

FIG. 3 (color online). Magnitude of orbital torque as a function of the radius of interacting spheres for the first (curve 1, blue) and second (curve 2, red) stationary orbits. The plus symbols indicate regions where the torque has opposite sign. The dashed lines indicate the analytical predictions based on Eq. (4) for Rayleigh particles. The calculations are for silica spheres in water excited with a plane wave of intensity 50 mW/μm^2 and wavelength in vacuum $\lambda = 532$ nm. The black line shows the magnitude of torque due to Brownian force at 290 K in the first stationary orbit. The inset depicts the symmetric potential energy landscape and the trajectory of a bound particle due to nonconservative orbital torques.

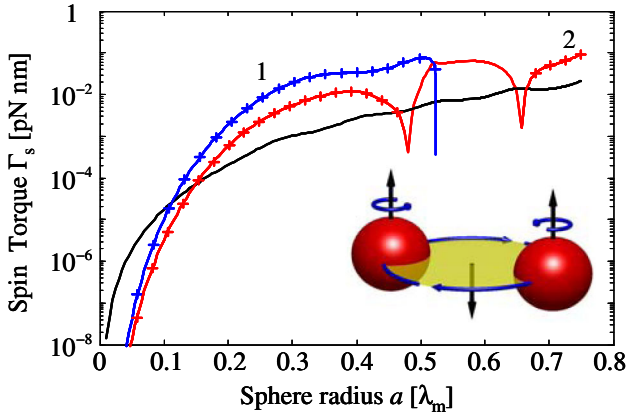

FIG. 4 (color online). Magnitude of spin torque Γ_s as a function of the radius of interacting spheres for the first (curve 1, blue) and second (curve 2, red) stationary orbits. The plus symbols indicate regions where the torque has opposite sign. The calculations are for the same conditions as in Fig. 3. The black line shows the magnitude of absorption-induced spin torque of one silica sphere with refractive index $n_i = 1.59 + 10^{-7}i$.

parameters, the spin torque increases with the particle size but, similar to the orbital torque, the sense of rotation is not always the same. Examining the two types of torques in Figs. 3 and 4, one can see that the spin and orbital torques have opposite directions for small particles but their behavior becomes more complicated when the sizes increase.

It is instructive to compare the magnitude of OB spin torque with the optical torque exerted on a particle due to its intrinsic absorption. The later can be estimated as $\Gamma_{\text{abs}} = |E_I|^2 a^2 Q_{\text{abs}}/4k$ [21], where Q_{abs} is the absorption coefficient. Estimations based on typical values for absorption in silica are shown in Fig. 4, and, as can be seen, spin torque dominates for $a \geq 0.1\lambda_m$. Notably, because the OB spin torque does not necessarily have the same direction as the excitation handedness while the torque due to absorption is always in the same direction, the two torques can combine to increase or cancel the net rotation.

Finally, one should note that the magnitudes of the orbital and spin rotations of OB particles may be affected by the surrounding medium. In fluids, in addition to the influence of viscosity on forces and torques, hydrodynamic coupling may occur between closely placed particles. For a sphere of radius $a = 0.4\lambda_m$ and an intensity of 50 mW/μm^2 in the Rotne-Prager approximation [22] one finds that, in the first stationary orbit, the orbital and spin angular velocity in water are $\Omega_o = 17$ rad/s, $\Omega_s = -2.6$ rad/s, respectively. It is worth mentioning that for these specific parameters, the liquid flow created by the orbiting spheres greatly affects their spin rotation forcing them to rotate in opposite direction with respect to acting torque Γ_s (as indicated by minus sign). In fact, the ratio between spin and orbital angular velocities can be optically modified. This external control together with the hydrodynamic coupling may be used to detect the presence of otherwise hardly noticeable spinning motion of OB spheres.

In conclusion, we have demonstrated that optical interaction forces can lead not only to binding, but also to complex rotations. The interplay between conservative and nonconservative forces constitutes a new mechanism to induce torques on spherically symmetric, optically isotropic, and lossless objects. The bound system discussed here constitutes a new kind of ''optical matter'' having its mechanical properties strongly coupled to the exciting radiation.

We found that when the incident field is linearly polarized, the torques are mostly conservative and affect only the transient behaviors. For circular polarization on the other hand, the nonconservative torques are significant and lead to nontrivial phenomena. In particular, bound systems can rotate not only around the common center of but also around their own axes. In the intermediate case of elliptically polarized light, the conservative torque will determine a transient orbital motion, whereas the nonconservative one will lead to a continuous spin rotation. The whole system can be seen as a ''nanomixer'' with complex mutual rotations of constituents. The direction and speed of these rotations can be dynamically controlled through the intensity, state of polarization, and spatial profile of the incident radiation. Our estimations indicate that effects are easily observable under reasonable environmental conditions.

This work was partially supported by the Air Force Office of Scientific Research and by the Army Research Office.

[1] A. Ashkin, Phys. Rev. Lett. **24**, 156 (1970).
[2] M. M. Burns, J.-M. Fournier, and J. A. Golovchenko, Phys. Rev. Lett. **63**, 1233 (1989).
[3] S. A. Tatarkova, A. E. Carruthers, and K. Dholakia, Phys. Rev. Lett. **89**, 283901 (2002).
[4] J. Rodríguez and D. L. Andrews, Opt. Lett. **33**, 2464 (2008).
[5] T. M. Grzegorczyk, B. A. Kemp, and J. A. Kong, Phys. Rev. Lett. **96**, 113903 (2006).
[6] K. Miyakawa, H. Adachi, and Y. Inoue, Appl. Phys. Lett. **84**, 5440 (2004).
[7] M. Dienerowitz, M. Mazilu, P. J. Reece, T. F. Krauss, and K. Dholakia, Opt. Express **16**, 4991 (2008).
[8] M. E. J. Friese, T. A. Nieminen, N. R. Heckenberg, and H. Rubinsztein-Dunlop, Nature (London) **394**, 348 (1998).
[9] Y. Roichman, Bo Sun, A. Stolarski, and D. G. Grier, Phys. Rev. Lett. **101**, 128301 (2008).
[10] J. Ellis and A. Dogariu, Phys. Rev. Lett. **95**, 203905 (2005).
[11] F. Depasse and J.-M. Vigoureux, J. Phys. D **27**, 914 (1994).
[12] S. K. Mohanty, J. T. Andrews, and P. K. Gupta, Opt. Express **12**, 2749 (2004).
[13] P. C. Chaumet and M. Nieto-Vesperinas, Opt. Lett. **25**, 1065 (2000).
[14] J. P. Barton, D. R. Alexander, and S. A. Schaub, J. Appl. Phys. **66**, 4594 (1989).
[15] V. Karásek, K. Dholakia, and P. Zemánek, Appl. Phys. B **84**, 149 (2006).
[16] A. G. Hoekstra, M. Frijlink, L. B. F. M. Waters, and P. M. A. Sloot, J. Opt. Soc. Am. A **18**, 1944 (2001).
[17] P. Chaumet and C. Billaudeau, Jpn. J. Appl. Phys. **101**, 03106 (2007).
[18] D. Haefner, S. Sukhov, and A. Dogariu, Phys. Rev. Lett. **102**, 123903 (2009).
[19] Because of the inconsistency in evaluating the field derivative, the approach in Ref. [11] leads to a force magnitude that decreases uniformly with R and, moreover, it depends not on $\text{Re}(\alpha)$, but on $\text{Im}(\alpha) \ll \text{Re}(\alpha)$.
[20] J. Keizer, *Statistical Thermodynamics of Nonequilibrium Processes* (Springer, Berlin, 1987), pp. 98–106.
[21] S. Chang and S. S. Lee, J. Opt. Soc. Am. B **2**, 1853 (1985).
[22] M. Reichert and H. Stark, Phys. Rev. E **69**, 031407 (2004).